

Local strain on a leachate collection pipe

R.W.I. Brachman, I.D. Moore, and R.K. Rowe

Abstract: Local strain measurements opposite gravel contacts and around a single isolated perforation are reported for a high-density-polyethylene pipe (320 mm outside diameter, 32 mm thick) typical of that commonly used as part of the leachate collection system in municipal solid waste landfills. Emphasis is given to examining the localized effect of coarse gravel contacts on pipe strain and the strain distribution around the perforation. The laboratory testing featured a cylindrical volume of soil with the pipe located in the middle with radially compressive stresses applied along the outer perimeter of the backfill. Two different backfill materials were used. When tested with medium sand backfill the pipe response was essentially uniform, indicative of the near-continuous support and loading provided by the sand. Large variations in local pipe strains were measured with coarse gravel backfill, such as that used in landfill leachate collection systems. Local bending induced by the discontinuous support and loading from the coarse gravel resulted in variations in circumferential and axial strains of over 40%. The local bending effects were not sufficiently large to produce circumferential tension in the pipe tested. A multiplication factor of 1.5 is suggested to account for increases in compressive strain from the coarse gravel. Measurements of surface strain around an isolated 32 mm diameter perforation revealed that a complex three-dimensional response is induced by the presence of the hole. Maximum strains near the hole were found to be 2.7 times larger than those distant from the perforation.

Key words: leachate collection pipes, HDPE pipes, leachate collection systems, landfill design.

Résumé : Les déformations locales mesurées sur les contacts opposés au gravier et autour d'une simple perforation isolée sont rapportées pour un tuyau de polyéthylène à haute densité (d'un diamètre extérieur de 320 mm et d'une épaisseur de 32 mm) typique de ce qui est couramment employé dans un système de collecte d'eau de percolation dans des sites de disposition de déchets solides municipaux. L'emphase est mise sur l'examen de l'effet localisé de contacts du gravier grossier sur les déformations au tuyau, et de la distribution de déformations autour de la perforation. Les tests en laboratoire ont impliqué un volume cylindrique de sol avec le tuyau situé au milieu, et avec des contraintes compressives radiales appliquées le long du périmètre extérieur du matériel de remblayage. Deux matériaux de remblayage différents ont été utilisés. Lorsque testé avec du sable de remblayage moyen, la réponse du tuyau a été essentiellement uniforme, ce qui est indicatif du support et du chargement quasi continus produits par le sable. De large variations dans les déformations locales sur le tuyau ont été mesurées lorsque le matériel de remblayage est un gravier grossier, tel que celui utilisé dans les systèmes de collecte d'eau de percolation des sites de disposition. Le fléchissement local induit par le support et le chargement discontinus provenant du gravier grossier a résulté en des variations de déformations radiale et axiale de plus de 40 %. Les effets du fléchissement local n'ont pas été suffisamment large pour produire une tension radiale dans le tuyau testé. Un facteur de multiplication de 1,5 est suggéré pour tenir compte des augmentations de la tension compressive provenant du gravier grossier. Les mesures de déformations de surface autour d'une perforation isolée d'un diamètre de 32 mm ont révélé qu'une réponse tridimensionnelle est induite par la présence du trou. Les déformations maximales près du trou ont été trouvées comme étant 2,7 fois plus grandes que celles éloignées de la perforation.

Mots clés : tuyau de collecte d'eau de percolation, tuyau de polyéthylène à haute densité, système de collecte d'eau de percolation, conception de sites de disposition.

[Traduit par la Rédaction]

Received September 9, 1999.

Revised manuscript accepted July 21, 2000.

R.W.I. Brachman.¹ Department of Civil and Environmental Engineering, University of Alberta, Edmonton, AB T6G 2G7, Canada.

I.D. Moore and R.K. Rowe. Department of Civil and Environmental Engineering, The University of Western Ontario, London, ON N6A 5B9, Canada.

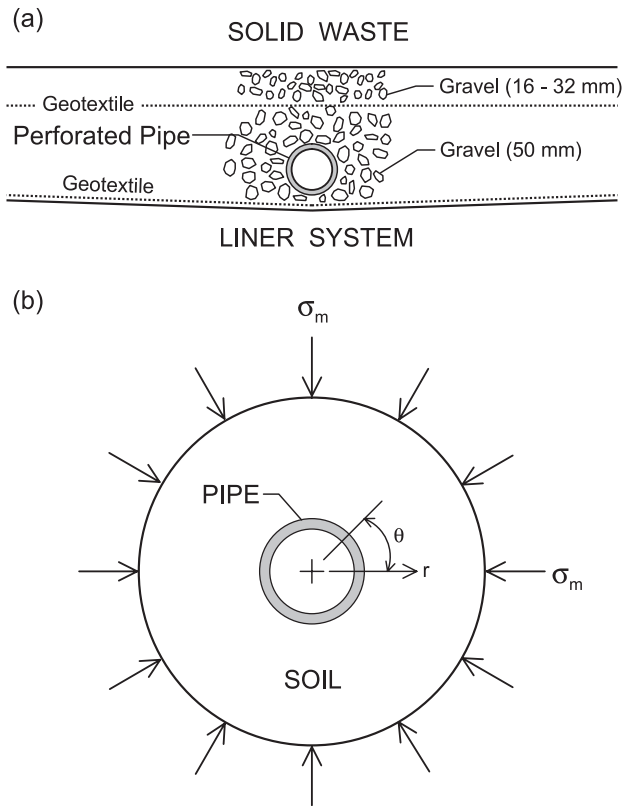
Written discussion of this article is welcomed and will be received by the Editor until April 30, 2001.

¹Author to whom all correspondence should be addressed (email: rbrachman@civil.ualberta.ca).

Introduction

Leachate collection systems are an important component of modern municipal solid waste landfills. They are intended to minimize the hydraulic gradient across the liner system (e.g., compacted clay and (or) geomembrane liner), and hence an operating leachate collection system is one factor that controls the migration of contaminants from the landfill. Collection systems also remove leachate from the facility, thereby reducing the contaminating lifespan of the landfill. A typical modern leachate collection system consists of perforated plastic pipes surrounded by coarse uniformly graded gravel (e.g., see Fig. 1a). Ensuring adequate structural per-

Fig. 1. (a) Cross section through a typical primary leachate collection system in a municipal solid waste landfill; (b) idealized loads acting on a soil-pipe system with distant boundary stress σ_m .



formance of these pipes is an important design issue for the leachate collection system.

It is now well known that the drainage materials of the leachate collection system can experience particulate, chemical, and biological clogging (e.g., Rowe et al. 1997). Clogging reduces the effectiveness of leachate collection and, other factors being equal, increases the contaminant transport from the landfill. The use of coarse gravel backfill and relatively large perforations are two design measures that are intended to minimize the clogging of the leachate collection system (see Rowe et al. 1997). However, these measures may lead to adverse service conditions for the pipe that are not experienced in typical buried pipe applications.

The large open void space and small surface area provided by the coarse gravel help to minimize biologically induced clogging. However, when the pipe is surrounded by coarse gravel, it will be supported at discrete points around the circumference rather than the more continuous support provided by other backfill materials (e.g., sand, well-graded gravel). Local bending stresses arising from the discontinuous support could potentially affect the structural performance of the drainage pipe.

The stress conditions within leachate collection pipes are further complicated by stress concentrations arising from the presence of perforations. These holes in the walls of the pipe, which are essential for the purpose of leachate collection, weaken the pipe compared to nonperforated pipe. Ideally, these holes should be sufficiently large to minimize the potential for clogging of the hole and also maximize the

effectiveness of cleaning efforts. However, at the same time, they should not be so large and so numerous that they compromise the structural integrity of the pipe. The magnitude of stress concentrations from coarse gravel backfill and perforations, and their effect on the mechanical performance of landfill drainage pipes, are presently unknown.

Two major issues related to coarse gravel backfill and perforations must be addressed. First, it must be established whether coarse gravel can be safely used as the drainage material around small diameter plastic pipes and, if so, the extent of the influence of local contact effects on the overall performance of the pipe must be quantified and incorporated in design procedures. Second, the influence of relatively large perforations on both the local response around the hole and the global response of the pipe must be established. Other technical issues requiring solution include the selection of an appropriate pipe wall thickness to limit local backfill contact effects, as well as the selection of the number, size, and spacing of perforations.

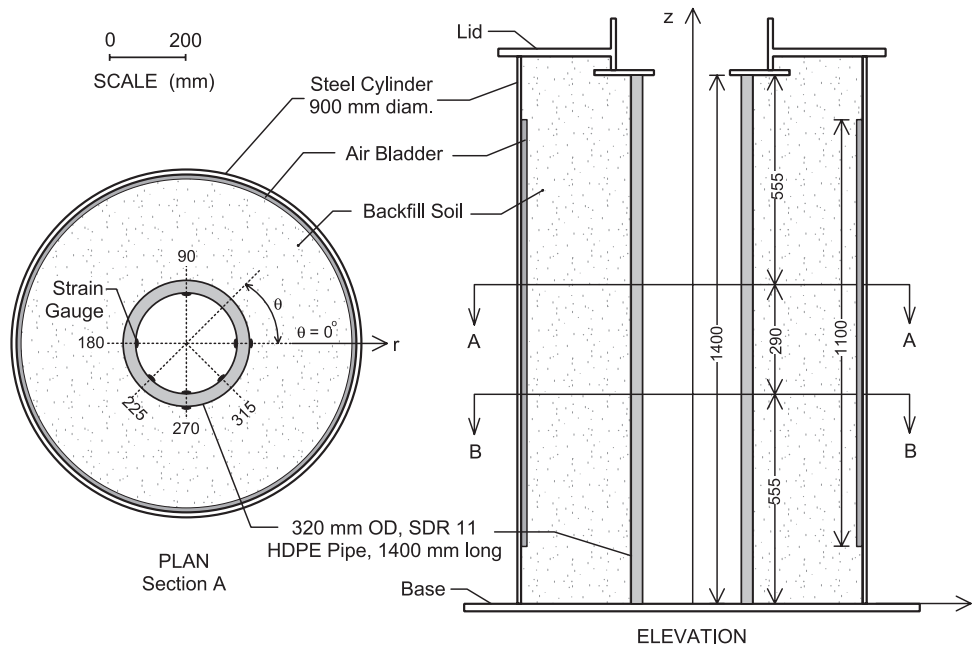
As a first step towards resolving these complex issues, the objective of this paper is to present results from three laboratory tests conducted with simplified boundary conditions to (i) study the localized effect of coarse gravel contact on pipe strain and (ii) examine the local strain distribution around single isolated perforations.

Results from a test with medium sand backfill and two tests with coarse gravel backfill are reported to study the effect of two different backfill materials on the structural performance of the pipe. The sand backfill essentially provides continuous support for the pipe, while the coarse gravel backfill results in discontinuous support and loading for the pipe. Measurements of surface strain opposite a zone of hand-placed stones in contact with the pipe are reported to study the local variations of strain from the coarse gravel backfill. Measurements of local strain around single isolated perforations are then presented for both sand and coarse gravel backfills to provide an estimate of strain concentrations in the pipe from the perforations. Preliminary recommendations for the design of landfill leachate collection pipes are given.

Laboratory facility for hoop compression testing

Leachate collection pipes are typically surrounded by a select backfill material (e.g., coarse gravel) and subject to loading from the solid waste overburden. The performance of the pipe is a function of both the stiffness of the pipe and the soil (i.e., soil-pipe system). Deep burial of a pipe leads to vertical and horizontal stresses (σ_v and σ_h) that act on the soil at some distance away from the pipe. A preliminary approach that may be used to simulate deep burial loading in the laboratory is to consider the response of the soil-pipe system when subject to the mean of the distant boundary stresses, σ_m (Fig. 1b), where $\sigma_m = \frac{1}{2}(\sigma_v + \sigma_h)$. Compressive hoop stresses develop in the pipe when the surrounding soil is subjected to the uniform, radial stress σ_m . This idealization does not model the biaxial earth pressures σ_v and σ_h that are expected to prevail under field conditions but is considered to be a useful prelude to more elaborate testing and analysis. Hoop compression tests involve simple boundary

Fig. 2. Plan and elevation view of hoop compression test facility showing location of instrumentation for pipe sample H1. Dimensions are in millimetres.



conditions, require a small volume of soil, and provide results that are relatively straightforward to model and interpret.

The laboratory tests were conducted in a facility similar to the one developed by Selig et al. (1994). The particular details of the hoop compression test cell used have been reported by Moore et al. (1996). Figure 2 shows plan and elevation sections through the test cell. Figure 3a is a photograph showing a plan view of the pipe, coarse gravel backfill, bladder and steel test cell. Essentially, a test specimen of pipe 1.4 m long was placed inside a 0.9 m diameter cylindrical steel test cell with the longitudinal axis of the pipe oriented in the vertical plane. The pipe was surrounded by the backfill soil. Once the lid of the cell was placed, a pressurized air bladder was used to apply a radial stress along the outer soil boundary. The bladder was made from nylon-reinforced chlorosulphonated polyethylene (1 mm thick) that was chemically seamed around the perimeter to form a sealed bag. The pressure applied by the bladder is close to the free field uniform stress σ_m (the soil zone absent beyond the air bladder has a small effect on the stress condition). The pipe response (deformations and surface strains) were recorded as the bladder pressure was applied. The bladder pressure was applied in 50 kPa increments that were rapidly applied and then held constant for a 10 min duration. This sequence was repeated for each load step up to the maximum pressure for each test.

Three tests were conducted in the hoop compression cell, denoted as tests H1, H2a, and H2b. Table 1 summarizes the important details for these tests. Two specimens of pipe with an outer diameter (OD) of 320 mm and dimension ratio (SDR) of 11 (where SDR is the ratio of outside diameter to the minimum wall thickness) were tested and are referred to as pipes H1 and H2. These pipes were made with a polyethylene material with cell classification PE 345434C in accor-

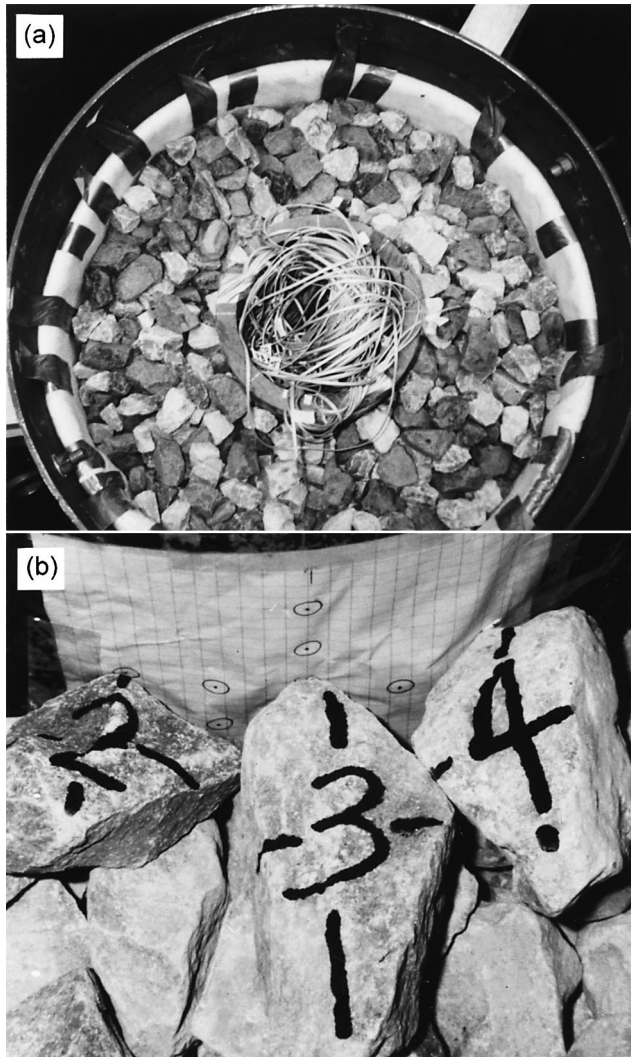
dance with ASTM D3350, and Class PE 3408 according to the Plastic Pipe Institute.

Backfill materials

Two different backfill materials were used in the testing. The material used for Test H1 was a poorly graded medium sand (SP). Leachate collection stone was used for tests H2a and H2b. This poorly graded coarse gravel (GP) consisted of large angular particles (crushed dolomitic limestone) with 70% finer than 51 mm sieve size and only 8% finer than 38 mm, and is now commonly specified as the drainage medium for leachate collection systems in Ontario, Canada. The two different backfill materials represent different loading conditions for the pipe. The support provided by the sand backfill will tend to be more uniform (the small sand particles provide almost continuous support around the pipe circumference), whereas the coarse gravel will provide non-uniform support (discontinuous support from much fewer contact points that are randomly distributed around the pipe circumference in field applications). The discontinuous support conditions arising from the coarse gravel backfill can be appreciated from Fig. 3b.

Backfilling procedures were selected to obtain uniform densities within the sand. The material was dumped in place, with the height of the fall constant for each lift. The material was placed in 150 mm thick lifts and was compacted imparting the same energy to each lift (dropping a 7 kg mass a vertical distance of 300 mm with three passes of compaction made for each lift). The densities were measured with a nuclear density meter that was calibrated with sand cone density tests to compensate for the close proximity of the steel and polyethylene. The sand was placed at an average bulk density of 1790 kg/m³ and an average water content of 3.4%. In accordance with typical field practice, the gravel

Fig. 3. (a) Plan view of hoop compression test cell showing pipe, coarse gravel, and bladder; (b) discontinuous support provided by coarse gravel.



was dumped into the cell with no compaction and was placed at an average bulk density of 1410 kg/m^3 . This was obtained by recording the net weight of the gravel in the cell and the volume it occupied.

Instrumentation

Strain gauges at Section A for pipe H1

The surface strains of the pipe were measured using electrical foil strain gauges. Stacked rosettes with a gauge length of 2 mm (Showa type N32-FA-2-120) were selected to provide strain measurements over a small region (important when investigating the effect of coarse gravel backfill).

The strain gauge layout for Test H1 was selected to measure the variation of pipe strain with the more continuous backfill support provided by the medium sand. Four rosettes were placed on the interior surface of the pipe around the circumference at $\theta = 0^\circ, 90^\circ, 180^\circ,$ and 270° , and two were placed on the outside at $\theta = 0^\circ$ and 270° at Section A ($z = 845 \text{ mm}$) as shown in Fig. 2. Two single gauges (also 2 mm

gauge length) were oriented in the circumferential direction at $\theta = 225^\circ$ and 315° at this section.

Strain gauges at Section A for pipe H2

Since the objective of tests H2a and H2b was to observe the effect of the coarse gravel backfill on local variations in surface strains of the pipe, a grid of strain gauge rosettes was located on a small portion of the interior surface of the pipe opposite a hand-placed gravel contact zone. Figures 4a and 4b show the strain gauge layout at Section A for pipe H2. The centre of the grid corresponds to the location $\theta = 270^\circ$ and $z = 845 \text{ mm}$. A grid marking the location of the gauges (see Fig. 3b) was used to position the gravel contacts on the pipe exterior in this region. Note that the circles drawn on the grid (Fig. 3b) represent the location of gauges on the interior surface of the pipe. Carbon paper was placed on the outside surface of the pipe to record the location and spacing of contact points from the gravel particles. Strain gauges were placed at 22.5 mm centre to centre spacings in the z -direction (locations G1, G2, G3, G4, and G5) and at 18 mm spacing in the θ direction (locations G6, G7, G3, G8, and G9) as illustrated in Fig. 4b. This interior grid of gauges permits the variations in pipe strains to be observed in both the circumferential and axial directions opposite the hand-placed contact region. Two rosettes were also located at opposite points G2 and G4 on the exterior surface of the pipe.

Strain gauges around a single perforation

As a first step towards the understanding of the effects of perforations on the pipe behaviour, another objective of these tests was to examine the local strain distribution around a single isolated perforation. Therefore pipes H1 and H2 each contained a single 32 mm diameter perforation located at Section B ($z = 555 \text{ mm}$, Fig. 2). The hole is located 290 mm (nine perforation diameters) away from Section A. Finite element analysis indicated that the perforation is expected to have a negligible (less than 2%) effect on the pipe stresses and deflections four perforation diameters (128 mm) away from the hole.

Figure 4c shows the location of the perforation at $\theta = 90^\circ$. Strain gauges were positioned around the hole on both the interior and exterior surfaces of the pipe. Three gauges were placed on the interior located at $0^\circ, 45^\circ,$ and 90° from the circumferential direction α , denoted as gauges P1, P2, and P3 in Fig. 4d. Two gauges were placed on the exterior surface, opposite to those on the inside at $\alpha = 0^\circ$ (P4) and 90° (P5). The centre of each gauge was located 4 mm from the edge of the perforation. A nonwoven geotextile was used to prevent the medium sand backfill from falling into the perforation.

Strain measurements with sand backfill

Circumferential strains

Circumferential strains (ϵ_θ) measured on the interior surface of the pipe at Section A ($z = 845 \text{ mm}$) are plotted in Fig. 5a. Strains are plotted with tensile strains as positive values (compressive strains are taken as negative) and expressed as microstrain ($\mu\epsilon$), where $1000 \mu\epsilon$ is 0.1% strain. The reported strains were averaged over the last 30 s of each increment and are the maximum strains for each load incre-

Table 1. Summary of hoop compression tests on 320 mm diameter, SDR 11, high-density-polyethylene pipes.

Test	Pipe	Backfill soil	Maximum applied pressure (kPa)	Average temperature (°C)
H1	H1	Uniformly graded medium sand	500	21
H2a	H2	Uniformly graded coarse gravel	250	23
H2b	H2	Uniformly graded coarse gravel	350	23

Fig. 4. (a) Location of strain gauges for pipe H2 at Section A; (b) view of strain gauge placement opposite stone contact zone (Section C) for pipe H2 from pipe interior; (c) location of strain gauges around a single 32 mm diameter perforation at Section B for both pipes H1 and H2; (d) Section D position of strain gauges around perforation — view from inside surface.

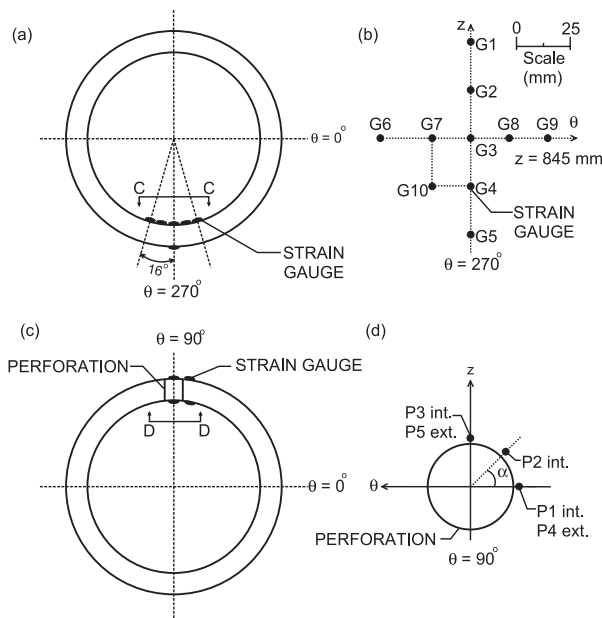
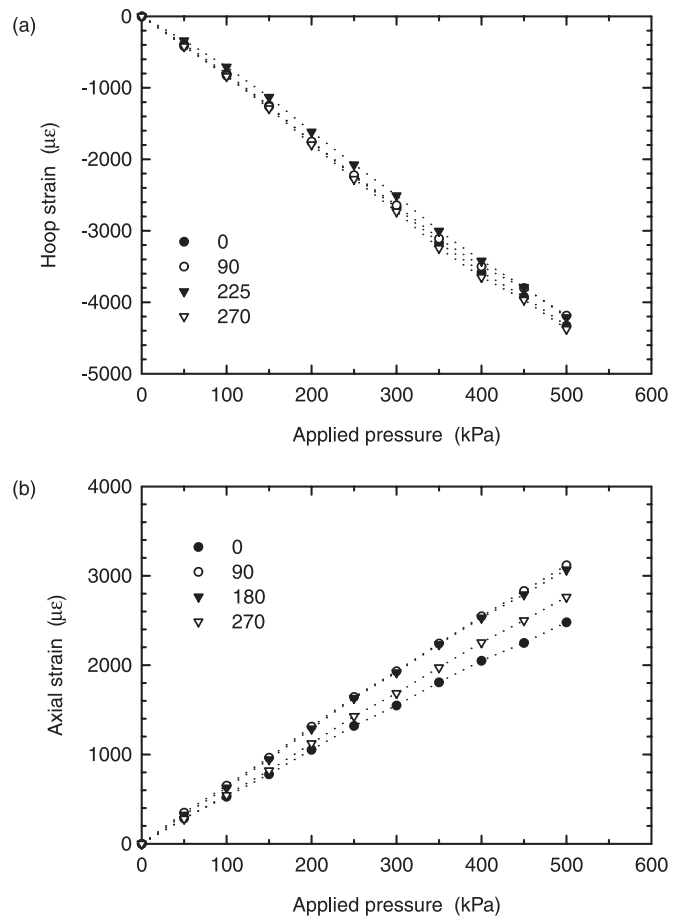


Fig. 5. Variation of (a) circumferential strain, ϵ_θ , and (b) axial strain, ϵ_z , measured in the circumferential direction at Section A during Test H1.



ment. The time-dependant response has been reported elsewhere (Brachman 1999).

Values are shown for ϵ_θ measured at four circumferential positions ($\theta = 0^\circ, 90^\circ, 225^\circ$, and 270°). The circumferential gauges located at $\theta = 180^\circ$ and 315° did not provide readings because of damaged lead wire connections.

The measured values of ϵ_θ became increasingly negative under hoop compression loading and are essentially linearly proportional to the applied radial pressure. This response was expected even though polyethylene is a visco-elastic material (for the strain levels tested here), since testing a visco-elastic material at a constant load increment (50 kPa every 10 min was used) results in strains that are linearly proportional to pressure (Moore and Hu 1995).

An average value of circumferential strain of $-4350 \pm 100 \mu\epsilon$ (where $\pm 100 \mu\epsilon$ is the 95% confidence interval of the mean) was found at an applied bladder pressure of 500 kPa. The four readings of circumferential strain agree quite well with each other (Table 2), having a standard deviation of only $90 \mu\epsilon$ at 500 kPa. This corresponds to a coefficient of variation (i.e., standard deviation \div mean) of 2% at this load

level. Only a 4% difference was observed between the maximum value (measured at 270°) and the minimum value (recorded at 90°) for this load level. Overall, the strain readings in the circumferential direction were radially symmetric, as expected for the medium sand backfill and uniform radial loading.

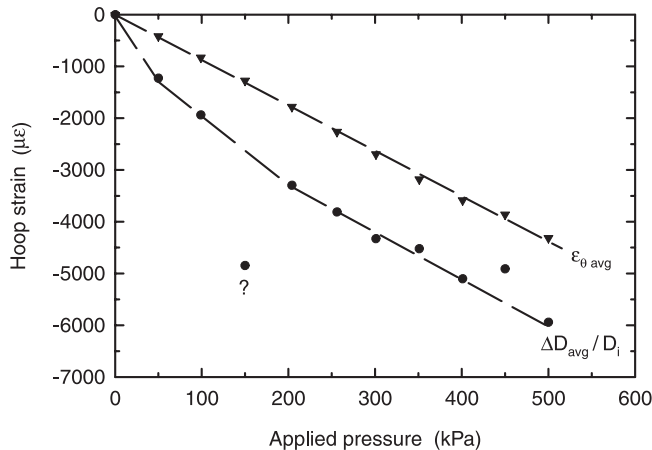
Axial strains

If plane strain conditions prevailed in the axial direction for both the soil and the pipe, axial strains corresponding to the axial elongation of the pipe would be zero. Such conditions are normally assumed to occur under deep burial, when conditions of long and prismatic geometry exist along the pipe axis. However, situations do arise where the pipe can experience axial elongation, for example at a thermal expan-

Table 2. Measured circumferential and axial strains (ϵ_θ and ϵ_z) at Section A during Test H1, reported at an applied bladder pressure of 500 kPa (strains reported to nearest 50 $\mu\epsilon$).

	Angular position around pipe, θ°					Mean	Coefficient of variation (%)
	0	90	180	225	270		
ϵ_θ ($\mu\epsilon$)	-4400	-4250	—	-4300	-4400	-4350	2
ϵ_z ($\mu\epsilon$)	2500	3150	3100	—	2800	2900	10

Fig. 6. Average circumferential strains measured with strain gauges compared with strains calculated based on measured deflections for Test H1.



sion joint or where the pipe enters a manhole. In such cases, axial extension of the pipe will lead to tensile axial strains and slightly larger pipe deflections relative to axial plane strain conditions. Tensile axial strains may lead to tensile axial stresses in the pipe, depending on the magnitude of the circumferential strains that also occur. Since tensile stresses may be more critical for polyethylene pipes — related to the long-term potential for stress cracking (e.g., see Mruk 1990) — consideration of nonzero axial strains is important for the performance of the pipe. Therefore, for the tests reported in this paper, it was decided to provide only nominal axial restraint for the pipe during these tests. It is noteworthy, however, that the circumferential stresses in the pipe under hoop compression loading do not vary for changes in axial restraint.

The axial strains (ϵ_z) measured on the inside surface at Section A are plotted in Fig. 5b. Values of ϵ_z are shown for locations $\theta = 0^\circ, 90^\circ, 180^\circ,$ and 270° . The axial strains are positive implying axial extension of the pipe and are comprised of two components. Most of the axial strains are attributed to the small degree of confinement in the axial direction. The deflection of the lid of the cell was found to be 3 mm at a bladder pressure of 500 kPa, corresponding to an axial strain of roughly 2100 $\mu\epsilon$. Another component of the observed axial strains arises from longitudinal bending of the pipe because the load is not applied across the entire pipe length (see Fig. 2).

The measured ϵ_z values increase to an average value of $2900 \pm 500 \mu\epsilon$ at 500 kPa of pressure. The axial strains vary more than the circumferential strains. There is a 20% difference between the minimum and maximum values measured

at $\theta = 0^\circ$ and 90° . The standard deviation was 300 $\mu\epsilon$ at an applied bladder pressure of 500 kPa, yielding a coefficient of variation of 10%. This variation probably arises because of slight bending in the axial direction arising from small variations in backfill stiffness that tends to reduce the axial strains at $\theta = 0^\circ$ and 270° and increase the values at $\theta = 90^\circ$ and 180° .

Strain gauge stiffening

The potential that the strain readings can be affected by the presence of the gauge itself is acknowledged (e.g., Beatty and Chewning 1979). This arises since the stiffness of the gauge (metal foil, polymer backing and glue) is similar to that of the polyethylene. The effect of the gauge stiffness upon the local strain readings may be quantified by comparing circumferential strain values measured using the strain gauges with values of strain calculated from measured deflections. For axisymmetric conditions, the strains on the inside surface of the pipe can be expressed as $\epsilon_\theta = \Delta D/D_i$, where D_i is the inside diameter of the pipe. The deflections of the pipe were measured using a laser analog sensor and have been reported elsewhere (Brachman 1999).

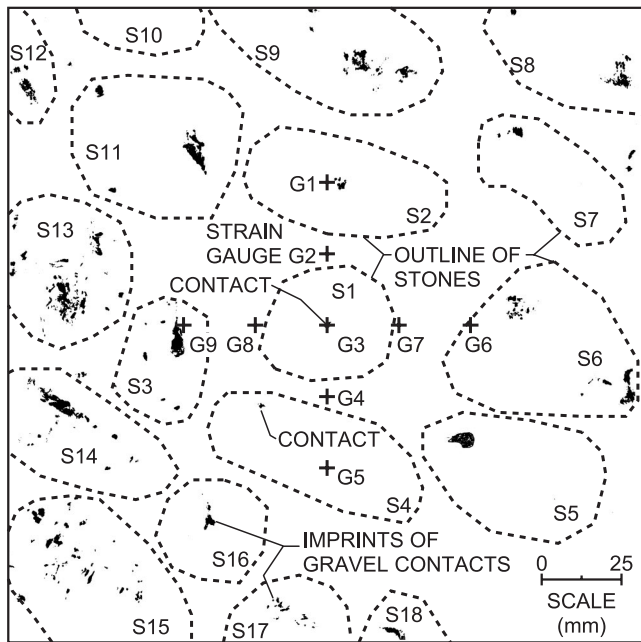
Figure 6 shows that the average strain measured with the strain gauges ($\epsilon_{\theta, avg}$) is consistently smaller in magnitude than the strain computed from the average diameter change ($\Delta D_{avg}/D_i$). Apart from some scatter of the values based on deflections at pressures of 150 and 450 kPa, the two curves exhibit similar trends. At an applied bladder pressure of 500 kPa the strain gauges measure only 73% of the circumferential strain calculated based on deflections. The strain gauge readings are consistently smaller because of a reinforcing effect provided by the gauge that results in a local reduction in the strain field beneath the gauge. Based on this figure, surface strain readings on polyethylene obtained from electrical foil strain gauges will be corrected for this stiffening effect by multiplying the measured strains by a correction factor of $1/0.73 = 1.4$. For the remainder of this paper, comparisons are made based on measured (uncorrected) strain values for studying the variations induced by the stone. Estimates of pipe stresses (based on measured strains) are corrected for the stiffening effect.

Local strain measurements with coarse gravel backfill

Nature of gravel contacts

The location of gravel contact points opposite the strain gauge grid for Test H2a are shown in Fig. 7. This information was obtained from the imprint of the carbon paper placed on the outside surface of the pipe. The locations of

Fig. 7. Gravel contact points on pipe exterior opposite strain gauges at Section A for Test H2a.



gravel contacts in this region recorded with photographs during careful exhumation of the gravel after the test are also shown in Fig. 7 to aid interpretation of the measured strain results.

The nature of the contacts between the gravel particles and the pipe varied widely with differing size, shape, and spacing as shown in Fig. 7. At some locations, only a single sharp contact occurred between the pipe and the gravel particle, like those for stones S1 or S7. At most other locations each gravel particle imposed many contacts on the pipe. A long and narrow trace was left by stone S14, since it made contact with the pipe along an edge of the stone, whereas a flatter surface of stone S15 rested against the pipe producing many discrete contacts. Since the pipe is both loaded and supported at the contact locations, large variations in local pipe response were expected given the complex nature of gravel contacts around the pipe exterior.

Measured strains

Surface strains from Test H2a are now considered to examine the effect of coarse gravel backfill on local pipe strains. Circumferential and axial strains measured opposite the hand-placed gravel contact zone are plotted in Figs. 8 and 9. The maximum applied pressure for this test was limited by the failure of the bladder at 250 kPa.

Variations in circumferential strain

Figures 8a and 9a reveal that large variations in circumferential strain were measured over a small portion of the interior surface of the pipe. The variation of ϵ_θ along the circumferential direction of the strain gauge grid is plotted in Fig. 8a showing the strains measured at points G9, G8, G3, G7, and G6 (see Fig. 7 for gauge location). A 38% difference in ϵ_θ between the maximum G7 and the minimum G9 compressive strains was found at 250 kPa. Variations of

ϵ_θ along the axial direction of the strain gauge grid are plotted in Fig. 9a for points G1, G2, G3, G4, and G5 of the grid, showing a 27% difference between the maximum G2 and the minimum G5 values at 250 kPa. Since the circumferential strain readings from the test with sand backfill (H1) demonstrated that consistent strain readings could be reproduced under axisymmetric conditions (with a maximum difference of only 4%), the observed variations in circumferential strain recorded during Test H2a can therefore be attributed to the discontinuous loading and support imposed by the coarse gravel. Clearly, coarse gravel backfill has a large influence on local pipe strains.

Description of local bending effects

Coarse gravel loads and supports the pipe at discrete points around the pipe exterior. This leads to local bending effects that produce the variations in results shown in Figs. 8 and 9. For the pipe tested, two factors that dominate the local bending effects are the spacing between contacts and differences between contact forces. Both of these factors are related to the size (relative to the pipe), shape and arrangement of the gravel particles and interactions between individual gravel particles.

Local bending is predominantly induced because of spacing between gravel contacts. If the contact forces were assumed to be equal and were equally spaced around the pipe, then on the interior surface of the pipe local bending would produce maximum incremental tension opposite the contact and maximum incremental compression halfway between two contacts. In the limit of only two diametrically opposed contacts around the pipe, maximum tension is opposite the contact and maximum compression on the pipe interior is halfway between the two contacts. This situation is analogous to the circumferential conditions in the parallel plate test. In the other limit of many contacts around the pipe (i.e., uniform external radial pressure), the pipe response is uniform circumferential compression. The results of Test H1 were very similar to the latter case. The effects of local bending for the pipe and gravel tested lie in between these two limits of contact spacing. Differences in contact forces around the pipe would further increase any local bending effects.

Stress concentrations on the pipe exterior directly beneath gravel contacts may also have a significant influence on local pipe response, especially for very thin pipes, and are related to both contact spacing and contact force. For example, fewer contacts around the pipe for the same distant boundary stress (i.e., σ_m in Fig. 1b) would result in a greater force per contact and hence larger stresses beneath the contact. Some slight permanent indentations from the gravel contacts were observed on the exterior surface of the pipe after testing. However, no severe damage from gravel impingement was noticed.

Correlation of strain and contact location

Examination of the test results recorded in Figs. 8a and 9a reveals that no circumferential tension was measured. For the coarse gravel tested, this particular pipe is thick enough such that the local bending effects are not sufficiently large to lead to circumferential tensile strains in the pipe. The lo-

Fig. 8. Variation of (a) circumferential strain, ϵ_θ , and (b) axial strain, ϵ_z , measured in the circumferential direction of the grid at Section A during Test H2a.

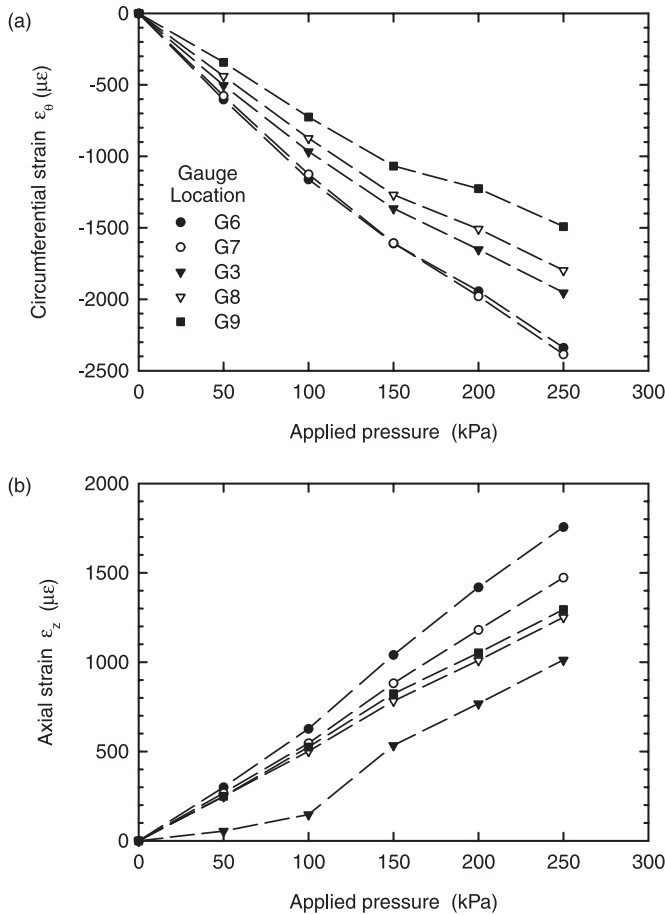
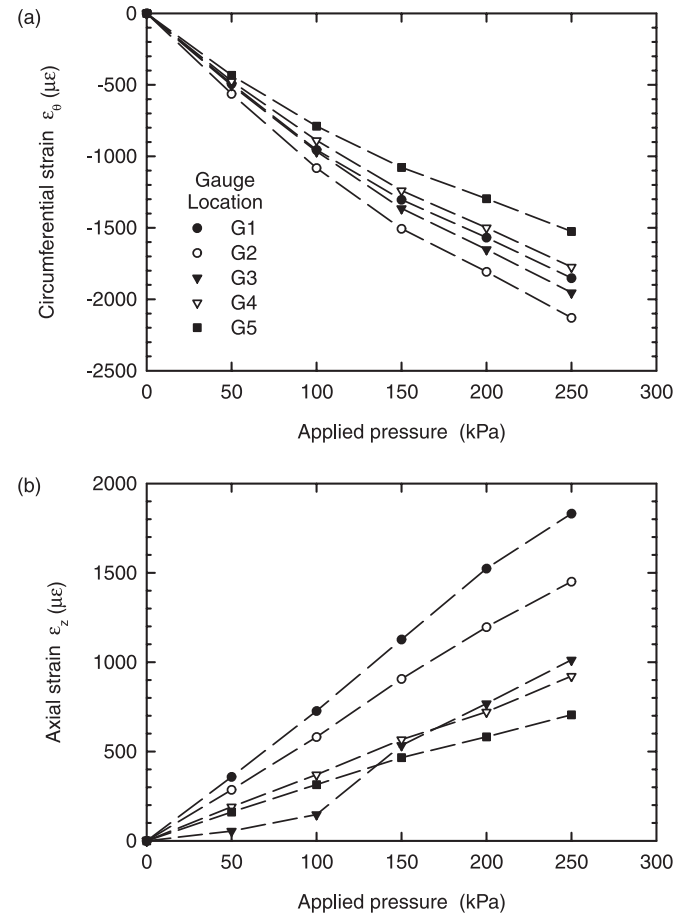


Fig. 9. Variation of (a) circumferential strain, ϵ_θ , and (b) axial strain, ϵ_z , measured in the axial direction of the grid at Section A during Test H2a.



cal bending effects, however, result in both increases and decreases in circumferential compression.

The largest compressive strains were measured at locations G6 and G7. Since these two points were located in between two widely spaced gravel contacts (Fig. 7), the large compressive strains are consistent with large incremental compression on the inside surface of the pipe from local bending. Large circumferential compression was also measured at G2, again, a point in between gravel contacts.

The smallest compressive hoop strain was found at location G9, directly opposite a gravel contact. The large incremental tension from local bending at this location produces a small compressive strain measurement. The close proximity of other gravel contacts near G9 (see Fig. 7) may also contribute to smaller compression at this point.

At the other locations, the strain measurements are not solely related to contact location. It is believed that variations in contact force at each gravel contact produces additional local bending. This complicates interpretation of the local pipe response, since the magnitude of the contact forces are unknown. For example, values at G1 and G3 (opposite contacts) are similar to measurements at G4 and G8 (between contacts).

Similar observations can be made for maximum measured axial strains. The largest axial strain was measured at location G1 (Fig. 9b). Since axial strains are tensile (resulting

from the axial boundary conditions), the maximum tension was expected directly opposite a gravel contact because local bending between contacts would produce incremental tension on the pipe interior opposite the contact.

Quantification of variations induced by coarse gravel

Considering the ten strain measurements of the grid together yields a mean circumferential strain of $-1900 \pm 200 \mu\epsilon$ at 250 kPa. A coefficient of variation of 16% was found for these measurements. The maximum recorded strain was near 1.3 times the mean value, similar to the ratio of mean to the minimum value. Axial strains varied more than the circumferential strains with the ten measurements, yielding a mean of $1300 \pm 300 \mu\epsilon$ and a coefficient of variation of 30%.

The same pipe specimen was tested again (H2b) with conditions nearly identical to Test H2a. Fewer gauges of the grid shown in Fig. 4b were monitored to also permit measurements of strain around the single perforation. The results between tests H2a and H2b were not statistically different at the 95% significance level (using a *t*-test distribution), thus permitting a valid comparison of measured values between the two tests.

The strains recorded during tests H2a and H2b are compared in Table 3 at an applied pressure of 250 kPa. Results between the two tests are very similar, since the gravel particles opposite the grid of strain gauges were hand placed in a

Table 3. Circumferential and axial strains (ϵ_θ and ϵ_z) opposite instrumented gravel contact zone measured during tests H2a and H2b, reported at an applied bladder pressure of 250 kPa (strains reported to nearest 50 $\mu\epsilon$).

Location	Test H2a		Test H2b	
	ϵ_θ ($\mu\epsilon$)	ϵ_z ($\mu\epsilon$)	ϵ_θ ($\mu\epsilon$)	ϵ_z ($\mu\epsilon$)
G1	-1850	1800	-1850	1700
G2	-2100	1450	-2200	1500
G3	-1950	1000	-2150	1200
G4	-1800	900	—	—
G5	-1500	700	-2000	1000
G7	-2350	1750	—	—
G7	-2400	1500	—	—
G8	-1800	1250	-1700	1500
G9	-1500	1300	-1400	1700
G10	-2000	1000	—	—
Mean	-1900	1300	-1900	1400
Coefficient of variation (%)	16	29	16	20

nearly identical manner. If the stones were placed in a random manner in each test, then the results from different tests would be expected to be different. For the fewer number of measurements during Test H2b, the mean circumferential strain was $-1900 \pm 300 \mu\epsilon$ with a coefficient of variation of 16%, while the mean axial strain was $1450 \pm 300 \mu\epsilon$ (20% coefficient of variation), both at a pressure of 250 kPa.

The coarse gravel backfill resulted in variations in strain, but not changes in the sign of the strain (i.e., in the circumferential direction, either increases or decreases in compressive strains occurred, but not tensile strains). One approach to account for these variations during pipe design may be to multiply the average strain ϵ_{calc} (obtained, say, from an analytical solution) by a strain magnification factor F_{gr} obtained from laboratory tests such as tests H2a and H2b to provide an estimate of the maximum compressive strain ϵ_{max} , viz.,

$$[1] \quad \epsilon_{max} = \epsilon_{calc} F_{gr}$$

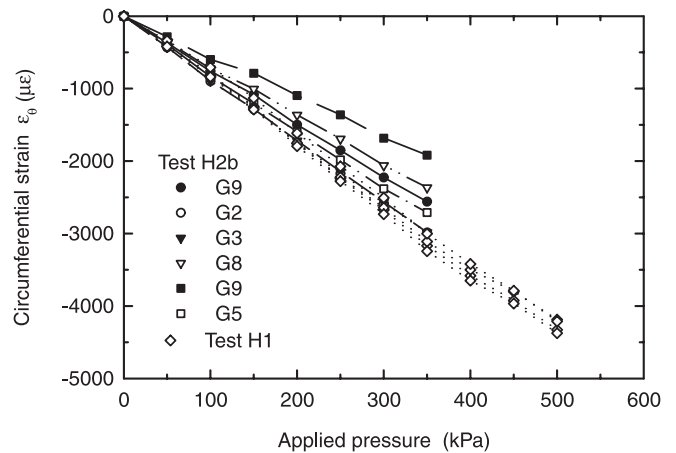
Based on the limited data, a strain magnification factor of 1.5 is suggested to account for increases in compressive strain from local bending effects.

Comparison of tests H1 and H2b

The strains measured at Section A during Test H2b are plotted in Fig. 10a against the applied bladder pressure. Also shown in these plots are the measured strains at Section A from Test H1. Overall, the responses of both backfill materials and the pipe are essentially linear over the applied pressures tested.

The variation in circumferential strains due to the gravel backfill is evident from the data in Fig. 10. The circumferential strains with gravel backfill are 16% smaller, on average, than those for the sand backfill. At 350 kPa, the mean circumferential strain from six readings was $-2600 \pm 400 \mu\epsilon$ with gravel backfill, while $-3100 \pm 160 \mu\epsilon$ was recorded for the sand backfill. This difference between the two means is statistically significant at the 95% level, indicating a slightly stiffer response of the gravel when tested in hoop compression relative to the sand at this particular density.

Fig. 10. Circumferential strains measured at Section A during tests H1 and H2b.



The observation of a stiffer response for the gravel compared with the sand is similar to what was found when considering the mean response of the pipe when tested under biaxial earth pressures (i.e., vertical stresses, σ_v , greater than horizontal stresses, σ_h) (Brachman et al. 2000). However, they also found greater strains with coarse gravel backfill than for sand when the overall response of the pipe was considered because of the difference in the lateral earth pressure coefficients (i.e., σ_h/σ_v) between the two backfill materials. Despite the difference in stress conditions between the uniform radial pressures of the hoop compression testing and the biaxial stresses expected in a landfill, the hoop compression results are useful to study the local strain variations induced by coarse gravel and around a single perforation.

Calculated stresses

The variation in pipe stresses resulting from the gravel backfill is also of practical interest. However, computation of stresses from measured strains is not trivial. Issues such as the strain gauge stiffening effect and the selection of a modulus value for polyethylene complicate the computations of stress from values of surface strain.

An estimate of the pipe stresses can be obtained based on the measured surface strains using Hooke’s Law for plane stress in the radial direction (i.e., $\sigma_r = 0$, which is valid on the inside surface of the pipe tested). An important consideration in estimating the pipe stresses based on measured strains is the selection of appropriate constitutive parameters for polyethylene. In general, the mechanical response of polyethylene is nonlinear and time dependent. The viscoplastic constitutive model of Zhang and Moore (1997), developed from samples taken from the same polyethylene pipe material as pipes H1 and H2, was used to estimate Young’s modulus for the appropriate strain levels and time. Secant moduli of 470, 440, and 400 MPa were used based on measured strains corresponding to applied bladder pressures of 250, 350, and 500 kPa, respectively. Poisson’s ratio of 0.46 and a strain gauge correction factor of 1.4 were used in all calculations.

The hoop and axial stresses calculated from the measured strains at Section A for tests H2a and H2b are summarized in Table 4 at an applied bladder pressure of 250 kPa. Compressive stresses are taken as negative values. Similar values

Table 4. Estimates of circumferential and axial stresses (σ_θ and σ_z) calculated from measured strains opposite instrumented gravel contact zone for tests H2a and H2b.

Location	Test H2a		Test H2b	
	σ_θ (MPa)	σ_z (MPa)	σ_θ (MPa)	σ_z (MPa)
G1	-0.8	0.8	-0.9	0.7
G2	-1.2	0.4	-1.2	0.5
G3	-1.2	0.1	-1.3	0.2
G4	-1.1	0.1	—	—
G5	-1	0	-1.3	0
G7	-1.3	0.6	—	—
G7	-1.4	0.3	—	—
G8	-1	0.3	-0.8	0.6
G9	-0.7	0.5	-0.5	0.9
G10	-1.3	0.1	—	—
Mean	-1.1	0.3	-1	0.5
Confidence level 95%	± 0.2	± 0.2	± 0.3	± 0.3
Coefficient of variation (%)	20	80	16	20

Note: Secant modulus of 470 MPa, Poisson's ratio of 0.46, and a gauge correction factor of 1.4 were used in the calculations. Stresses are reported for an applied bladder pressure of 250 kPa. Compressive stresses are negative.

of pipe stresses are obtained for the two tests. The mean hoop stress from Test H2a was -1.1 ± 0.2 MPa, with values varying from -0.7 to -1.4 MPa. While the local bending stresses arising from the gravel backfill cause these variations (50% difference between maximum and minimum), the pipe is sufficiently thick (for this particular coarse gravel and pipe diameter) such that tensile stresses do not exist in the hoop direction when subject to axisymmetric radial stresses. Tensile stresses are typically a greater concern for polyethylene pipes, related to the long-term potential for stress cracking. When the pipe is subject to biaxial earth pressures (i.e., where vertical pressures are greater than horizontal pressures), tensile hoop stresses may occur in the pipe. In this case, local bending effects imposed by the coarse gravel backfill will likely lead to larger tensile stresses at some locations. The effects of the local bending stresses on the stresses in the pipe when subject to the more realistic case of biaxial earth pressures have been studied by Brachman (1999).

Axial stresses are tensile with a mean of 0.3 ± 0.2 MPa at 250 kPa pressure. These tensile stresses are well below allowable working stresses of 4.3 MPa (hydrostatic design stress) for these pipes. However, these results do show that tensile axial stresses can occur if little axial restraint is provided to the pipe. Axial tensile stresses are increased by the local bending effects from the coarse gravel.

Local strains around a single isolated perforation

Test H1 — sand backfill

Strains measured around a single isolated perforation located at Section B (see Figs. 2 and 4c) with sand backfill are

presented in Fig. 11 for an applied pressure of 500 kPa. To study the perforation response, it is convenient to define another coordinate system with its origin coincident with the centre of the perforation, characterized by radius ρ and angle α from the circumferential direction (Fig. 4d). Figure 11 gives the strains measured tangential (Figs. 11a and 11b) and normal (Figs. 11c and 11d) to the hole for different angular positions around the hole. Results are shown for values measured on both the inside and outside surfaces of the pipe and are reported to the nearest $\pm 50 \mu\epsilon$.

Variations in strain around perforation

The strains plotted in Figure 11 are indicative of elliptical deformations of the circular hole. The inferred deformed shape of perforation is plotted in Fig. 11e. At $\alpha = 0^\circ$, the deflection is towards the centre of the hole, while at $\alpha = 90^\circ$, the deflection is away from the centre of the hole. These deformations produce tensile strains at $\alpha = 0^\circ$ and compressive strains at $\alpha = 90^\circ$ tangential to the hole, and compressive strains at $\alpha = 0^\circ$ and tensile strains at $\alpha = 90^\circ$ normal to the hole.

Variations in strain through pipe thickness

Comparison of the strains measured on the interior and exterior surfaces of the pipe (Fig. 11) shows that they have a similar distribution around the hole; however, the magnitudes are substantially different. The variation in strain through the pipe thickness is a noteworthy observation suggesting a complex three-dimensional response of the perforation. Analysis of perforations using a simple approximation of a hole in a thin plate or cylindrical shell (for which solutions do exist) is not expected to capture the mechanics of this particular problem.

The variations in strain through the thickness of the pipe can also be explained by examining the deformed shape of the hole. Three-dimensional finite element analysis of this problem revealed that the inward deflection of the hole at $\alpha = 0^\circ$ is greater on the pipe interior than on the exterior, and that the outward deflection at $\alpha = 90^\circ$ is greater on the pipe exterior than on the interior, as illustrated in Fig. 11e. This results in greater tension at $\alpha = 0^\circ$ on the exterior and greater compression at $\alpha = 90^\circ$ on the interior, both tangential to the hole, and is consistent with the results shown in Figs. 11a and 11b. Normal to the hole, and at $\alpha = 0^\circ$, larger compression on the exterior and smaller compression on the interior occurs from bending effects in the plane P1–P4, while at $\alpha = 90^\circ$, larger tension on the interior and smaller tension on the exterior is caused by bending in the plane P3–P5. These observations are also consistent with the measured results (Figs. 11c and 11d).

Magnification of strain near perforation

One important issue for the design of landfill pipes is the magnification of strain around the perforation. Strains are expected to peak directly at the edge of the perforation and then rapidly attenuate with increasing distance away from the hole. The strains measured during the tests are therefore not the maximum values near the perforation, since they were measured along a 2 mm gauge length centred 4 mm from the edge of the hole. Three-dimensional finite element analysis was used to compare the strain averaged over the

length of the gauge with the maximum strain at the edge of the hole.

The maximum measured compressive strain was recorded tangential to the single perforation on the inside surface at $\alpha = 90^\circ$. Results from the finite element analysis showed that the maximum strain at the edge of the hole strain at $\alpha = 90^\circ$ is 1.7 times larger than the value measured by the strain gauge. The maximum compressive strain around the hole can be compared with the strain measured distant from the hole (average of four values measured at Section A). The maximum compressive strain around the perforation is estimated to be 2.7 times larger than the strain distant from the hole.

Chambers and McGrath (1981) suggested the use of strain concentration factors of 2.3 for a circular hole in a smooth-wall pipe (like that considered here) in bending and 3.0 for a circular hole in uniform tension. The single perforation tested here is subject to both compressive and tensile stresses (in the circumferential and axial directions, respectively). Based on the limited measurements, it appears that a strain concentration factor of not less than 2.7 should be used for design purposes, and possibly that a concentration factor of 3.0 should be used.

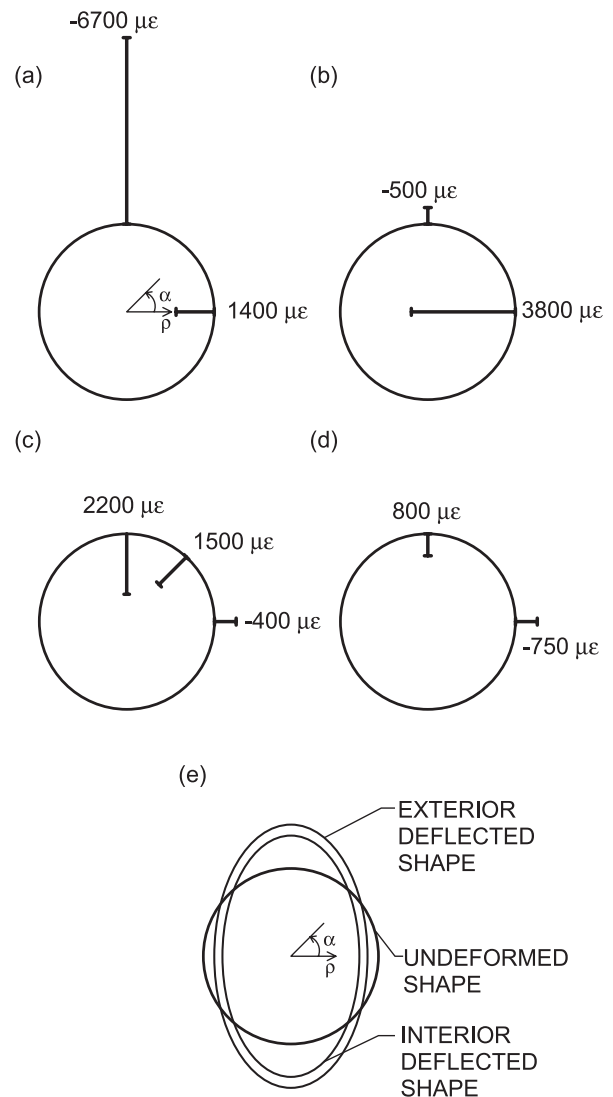
The strains around the perforation depend on both the circumferential and axial stresses distant from the hole. Large tensile strains at $\alpha = 0^\circ$ and compressive strains at $\alpha = 90^\circ$ occur because of the minimal axial restraint for the pipe during testing. Smaller strains would be expected around the hole for holes in pipes under plane strain axial conditions (where compressive axial stresses would occur distant from the hole). The strain concentration factor derived from this test can therefore be conservatively used for axial plane strain conditions. The condition examined here most closely approximates the condition near a concrete manhole where there is little axial restraint, or near an area where an expansion joint is left during construction.

Test H2b — coarse gravel backfill

Strains tangential and normal to the perforation for the case of coarse gravel backfill are presented in Fig. 12 at a bladder pressure of 350 kPa. The distribution of strains around the hole is similar to the pattern observed for sand backfill conditions. Again, an elliptical deformation shape of the hole occurs, producing a maximum compressive strain located at $\alpha = 90^\circ$ on the inside surface and tangential to the hole.

Local bending effects from the coarse gravel backfill further complicate the response around the perforation. Consequently, comparison of the strains around the perforation with values measured away from the hole is not as straightforward as for the case with sand backfill. Six values of circumferential strain opposite the hand-placed contact zone at Section A were averaged to characterize the strains distant from the perforation, yielding an average strain of $-2600 \pm 400 \mu\epsilon$ at 350 kPa. The measured value near the perforation was $-5500 \mu\epsilon$ at 350 kPa. When multiplied by 1.7 to account for the averaging of strain by the gauge, the maximum compressive value at the hole is 3.6 times the average distant value strain, which is larger than that observed with sand

Fig. 11. Strain tangential and normal to the perforation on the interior and exterior surfaces of the pipe for Test H1 with medium sand backfill at an applied bladder pressure of 500 kPa: (a) strain tangential to the hole on interior surface; (b) strain tangential to the hole on exterior surface; (c) strain normal to the hole on interior surface; (d) strain normal to the hole on exterior surface; and (e) inferred deformed shape of the perforation.



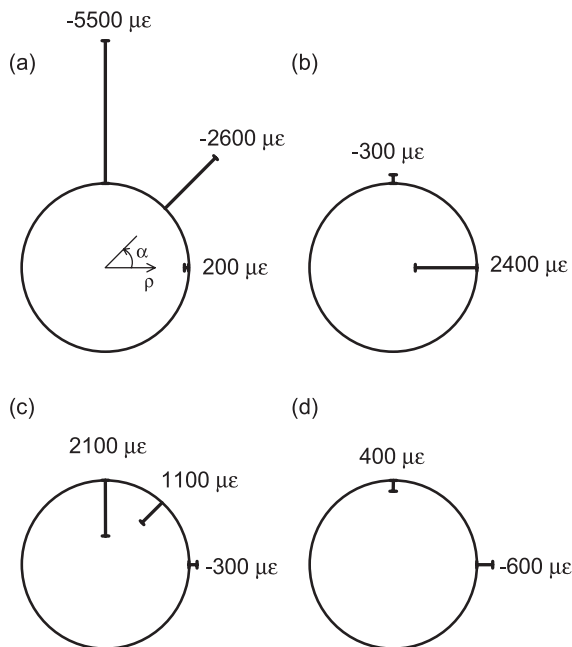
backfill. As expected, the coarse gravel backfill further complicates the strain response around the perforation.

During pipe design, the maximum strain at the perforation may be estimated by magnifying the strains distant from the hole by factors that separately account for effects from the coarse gravel backfill and the perforation, viz.,

$$[2] \quad \epsilon_{\text{perf}} = \epsilon_{\text{calc}} F_{\text{gr}} F_{\text{perf}}$$

where ϵ_{perf} is the maximum strain at the perforation, ϵ_{calc} is the calculated strain distant from the hole, F_{gr} is a strain magnification factor from the coarse gravel, and F_{perf} is a strain concentration factor from the perforation. Although additional testing is required, use of a strain concentration factor, F_{perf} , of at least 2.7 to account for the presence of the

Fig. 12. Strain tangential and normal to the perforation on the interior and exterior surfaces of the pipe for Test H2b with coarse gravel backfill at an applied bladder pressure of 350 kPa: (a) strain tangential to the hole on interior surface; (b) strain tangential to the hole on exterior surface; (c) strain normal to the hole on interior surface; and (d) strain normal to the hole on exterior surface.



hole in conjunction with a strain magnification factor from local bending effects, F_{gr} , of 1.5 is suggested for the preliminary design of pipes for the specific conditions tested (320 mm OD pipes with SDR of 11, perforation diameter of 32 mm, and nominal 50 mm coarse gravel).

Conclusions

The results of hoop compression tests for 320 mm OD, SDR 11, high-density-polyethylene pipes tested with medium sand and coarse gravel backfill materials were presented. The major conclusions from the test with medium sand backfill are as follows:

- Measured circumferential strains at different locations around the pipe were nearly identical (4% variation), which was expected given the radially symmetric loading conditions and the near-continuous support provided by the sand backfill. This demonstrated that consistent strain readings could be obtained; thus any variations in circumferential strain with coarse gravel can be attributed to the effect of the coarse gravel backfill.
- Tensile axial strains occurred in the pipe because axial restraint conditions were chosen to be closer to plane stress conditions and the load was not applied along the entire length of the pipe.
- A stiffening effect of strain readings using electrical foil strain gauges was observed and a simple correction factor of 1.4 based on measured pipe deflections was proposed.

The study of the effect of coarse gravel backfill on local pipe strains revealed the following:

- Circumferential and axial strains on the inside surface of the pipe opposite a number of hand-placed gravel particles varied by more than 40%.
- The measured variations occurred because of local bending effects induced from the discontinuous support and loading provided to the pipe by the coarse gravel. Local bending is from both the spacing between contact locations and the forces, which vary from contact to contact.
- For the nominal 50 mm coarse gravel tested, this particular pipe was thick enough that the local bending effects are not sufficiently large to lead to tensile circumferential strains.
- Maximum compressive circumferential strain on the pipe interior was measured at a point in between contacts where local bending produced large incremental compression.
- Minimum compressive circumferential strain was measured directly opposite contact locations where local bending produced large incremental tension.
- A strain magnification factor of 1.5 is suggested to account for increases in compressive strain from local bending effects for the particular pipe and coarse gravel tested.

Local strain measurements around a single 32 mm diameter perforation were also presented. These values were compared with strains measured distant from the perforation to study the effect of an isolated hole on the local pipe strains. For the specific conditions tested, the following are concluded:

- A complex three-dimensional response is induced around the perforation.
- The perforation deformed into an elliptical shape producing both compressive and tensile strains around the hole.
- The maximum compressive strain was found to be 2.7 times larger than those measured distant from the hole.
- Strains around the perforation were further complicated by local bending effects when coarse gravel backfill was used. For isolated perforations in pipes with coarse gravel backfill, use of strain concentration factor of at least 2.7 and a strain magnification factor of 1.5 (i.e., a combined magnification of 4.05) is suggested for the specific conditions tested.

Thus, from the available test data, it appears that nominal 50 mm coarse gravel and 32 mm diameter perforations can be safely used for landfill pipes (with a SDR of 11 or less), provided magnifications in pipe strains are accounted for during pipe design. Further work is required to guide the selection of appropriate pipe thickness to limit local backfill effects and the selection of the number, size, and spacing of perforations.

Acknowledgements

This research was funded by the Natural Sciences and Engineering Research Council of Canada. The assistance of Mr. A. Tognon with conducting the laboratory tests is gratefully acknowledged.

References

- Beatty, M.F., and Chewning, S.W. 1979. Numerical analysis of the reinforcement effect of a strain gauge applied to a soft material. *International Journal of Engineering Science*, **17**: 907–915.
- Brachman, R.W.I. 1999. Mechanical performance of landfill leachate collection pipes. Ph.D. thesis, Department of Civil and Environmental Engineering, The University of Western Ontario, London, Ont.
- Brachman, R.W.I., Moore, I.D., and Rowe, R.K. 2001. The performance of a laboratory facility for testing small diameter buried pipes. *Canadian Geotechnical Journal*, **38**: In press.
- Chambers, R.E., and McGrath, T.J. 1981. Structural design of buried plastic pipe. *Proceedings of the International Conference on Underground Plastic Pipe*. Edited by B.J. Schrock. American Society of Civil Engineers, New Orleans, La., pp. 10–25.
- Moore, I.D., and Hu, F. 1995. Significance of time dependent HDPE pipe response. *Proceedings of the 1995 Annual Conference of the Canadian Society for Civil Engineering*, Ottawa, Ont., pp. 555–564.
- Moore, I.D., Laidlaw, T.C., and Brachman, R.W.I. 1996. Test cells for static pipe response under deep burial. *Proceedings of the 49th Canadian Geotechnical Conference*, St. John's, Nfld., pp. 737–744.
- Mruk, S.A. 1990. The durability of polyethylene piping. *In Buried plastic pipe technology*. Edited by G.S. Buczala and M.J. Cassady. American Society for Testing and Materials, Philadelphia, Pa., STP 1093, pp. 21–39.
- Rowe, R.K., Quigley, R.M., and Booker, J.R. 1997. *Clayey barrier systems for waste disposal facilities*. E & FN Spon, London, England.
- Selig, E.T., DiFrancesco, L.C., and McGrath, T.J. 1994. Laboratory test of buried pipe in hoop compression. *In Buried plastic pipe technology*. Vol. 2. American Society for Testing and Materials, Philadelphia, Pa., STP 1222, pp. 119–132.
- Zhang, C., and Moore, I.D. 1997. Nonlinear mechanical response of high density polyethylene. Part I: experimental investigation and model evaluation. *Polymer Engineering and Science*, **37**(2): 404–413.

List of symbols

- F_{gr} strain magnification factor from gravel
 F_{perf} strain concentration factor from perforation
 OD outside diameter of pipe
 r radial direction from the centre of the pipe
 SDR standard dimension ratio (outside diameter/ minimum pipe thickness)
 z axial direction along the length of the pipe
 α orientation around perforation
 ΔD pipe diameter change
 ϵ_{θ} circumferential strain
 ϵ_{calc} pipe strain calculated from analytical solution
 ϵ_{max} maximum compressive strain
 ϵ_{perf} maximum compressive strain at perforation
 ϵ_z axial strain
 θ circumferential direction
 ρ radial direction from the centre of the perforation
 σ_h horizontal earth pressure
 σ_m mean boundary stress
 σ_v vertical earth pressure
 σ_z axial stress
 σ_{θ} circumferential (or hoop) stress